



Numerical investigation of heat transfer from heat sources placed in a horizontal rectangular channel

Ayla DOĞAN¹ , Mecit SIVRIOĞLU² , Senol BASKAYA²

¹Akdeniz University, Faculty of Engineering, Department of Mechanical Engineering, Antalya, TURKEY

²Gazi University, Faculty of Engineering, Department of Mechanical Engineering, Ankara, TURKEY

Abstract

In this study, three dimensional mixed convection heat transfer from discrete heat sources placed in a horizontal rectangular channel has been investigated numerically. 8x4 flush-mounted discrete heat sources were mounted on the lower and upper surfaces of the channel. Air is used as working fluid ($Pr \approx 0.7$). The heaters at the bottom and at the top wall were kept at a constant heat flux. Side walls, upper and lower walls are insulated and considered adiabatic. Nusselt number distributions and the effect of the Grashof number ($5.8 \times 10^6 \leq Gr^* \leq 2.3 \times 10^7$) and Reynolds number ($150 \leq Re \leq 971$) on the buoyancy-driven secondary flow have been investigated. Distributions of velocity vectors and temperature contours have been determined by the numerical method, and the results have been presented in detail. Governing equations were solved by the control volume method using suitable boundary conditions. The numerical parametric study was made for aspect ratio of $AR=8$, at various Reynolds and Grashof numbers.

Article info

History:

Received: 02.06.2020

Accepted: 02.09.2020

Keywords:

Electronic cooling, mixed convection, numerical study, heat sources.

1. Introduction

Mixed convection heat transfer in horizontal channels has received a considerable attention and has been applied in a wide range of engineering applications, such as heat exchangers, cooling of electronic equipment solar collectors, chemical processes and similar industrial applications. The most common methods applied for the cooling of electronic equipment comprise mixed convection using air or a liquid as the coolant fluid.

An earlier investigation on electronic cooling was conducted by Kennedy and Zebib [1]. They investigated heat transfer from discrete heat sources between horizontal parallel planes under mixed convection conditions. Four different local heat source configurations were studied numerically and experimentally. Incropera et al. [2] who had another earlier study investigated heat transfer from a single and an array of flush mounted heat sources for water and FC-77 in a rectangular channel. Numerical mixed convection in an inclined channel with discrete heat sources subjected to uniform heat flux was studied by Choi and Ortega [3].

Three-dimensional mixed convection heat transfer from an array of discrete heat sources in a horizontal

rectangular duct was studied numerically by Mahaney et al. [4]. The obtained results showed that the variation of the row-average Nusselt number with Reynolds number exhibits a minimum, suggesting that heat transfer may be enhanced due to buoyancy-induced secondary flow, by reducing the flow rate and hence the pumping requirements.

Doğan et al. [5] investigated experimentally mixed convection heat transfer in a top and bottom heated rectangular channel with discrete heat sources for air. The lower and upper surfaces of the channel were equipped with 8x4 flush-mounted heat sources subjected to uniform heat flux. Whole sides of the channel are insulated. The experimental study was made for an aspect ratio of (AR) 6, Reynolds numbers $955 \leq Re_{Dh} \leq 2220$ and modified Grashof numbers $Gr^* = 1.7 \leq 10^7$ to $6.7 \leq 10^7$.

Ozsunar et al. [6] investigated numerically mixed convection heat transfer in a rectangular channel under various operating conditions. They analyzed the effects of Grashof number, Reynolds number and inclination on mixed convection heat transfer. Air is used as the working fluid. A uniform heat flux was subjected to the lower surface of the channel, sidewalls are insulated and the upper surface is

*Corresponding author. Email address: ayladogan@akdeniz.edu.tr

exposed to the surrounding air. The numerical study was made for inclination angles $0^\circ \leq \theta \leq 90^\circ$, Reynolds numbers $50 \leq Re \leq 1000$, and modified Grashof numbers $Gr = 7.0 \times 10^5$ to 4.0×10^6 .

Numerical investigation of three-dimensional laminar mixed convection heat transfer in a vertical channel with an array of heated blocks, simulating electronic components, have been investigated by Amirouche and Bessaih [7]. The governing equations used in the problem were solved by the finite-volume method. Heated elements were kept at constant temperature. Calculations were performed for a wide range of Grashof numbers and Reynolds numbers. None heated block cases were also considered. The obtained results were compared with experimental data obtained for similar parameters.

Alami et al. [8] investigated numerically free convection heat transfer from electronic components in a horizontal channel with slots. The governing equations were solved using a control volume method, and the SIMPLEC algorithm was used for treatment of the pressure-velocity coupling. The results were obtained for Rayleigh numbers ($10^4 \leq Ra \leq 8 \times 10^5$), Prandtl number ($Pr=0.72$), opening width ($C=0.15$), block gap ($0.15 \leq RD \leq 1.0$), and block height ($B=0.5$).

In their experimental study, Dogan and Öney [9] investigated convective heat transfer in a horizontal channel with expanded heat sources with aluminum foam heat sinks. In order to investigate the effects on electronic element performance, they determined their effects on heat transfer by placing aluminum foam heat sinks on copper heaters in discrete form. The heat transfer results obtained for the empty surface and the foamed surface were compared and it is seen that with the use of aluminum foam heat sinks increases the heat transfer rate between approximately 36% and 70%.

Doğan and Ozbalcı [10] have experimentally investigated the natural convection heat transfer from porous materials mounted in an inclined rectangular duct. The experiments were made for different Rayleigh Number range from 2.03×10^7 to 1.33×10^8 and the channel inclination angles were varied from 0° to 90° . They determined that duct inclination angles and the use of porous materials have important effects on heat transfer.

In the literature reviews, it was seen that there are very few articles that modeling electronic elements

both separately and numerically. The present numerical study reports the initial results of a numerical investigation of mixed convection heat transfer in a horizontal channel, which is discretely heated at the upper and lower and the remaining channel surfaces are insulated. The numerical results have been compared with the experimental results in a previous detailed study by Dogan [11].

2. Numerical Model

The system under consideration is a three-dimensional channel model. The geometry and coordinate system of the horizontal channel with rectangular cross section used in the present study are depicted in Figure 1. Each of the lower and upper surfaces of the channel are equipped with 8×4 flush mounted heat sources, subjected to a uniform heat flux. The remaining sides of the channel are assumed to be completely insulated.

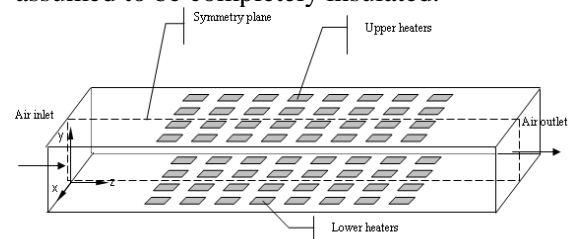


Figure 1. Schematic illustration of the computational domain

In this study, basic conservation equations defining the problem were solved with PHOENICS (Parabolic Hyperbolic or Elliptic Numerical Integrated Code Series) code working with the finite volume method. PHOENICS is a program that simulates heat and mass transfer, fluid mechanics, chemical reactions and similar events (Rosten and Spalding [12]). This CFD code provides iterative numerical approaches for solving nonlinear partial differential equation sets. Numerical solution procedure commonly used SIMPLE is an advanced form of the algorithm (Spalding [13]). Hybrid method was used for convection-diffusion transport. Equation sets are solved by TDMA (Tridiagonal-Matrix-Algorithm) algorithm.

Reliability criteria must be met in studies using the CFD method. In general, in CFD applications, for the solution results to give real values, the solution must be independent of the cell structure, and basic conservation equations must be satisfied. In this study, a $21 \times 20 \times 99$ cell structure was determined to be appropriate.

3. Mathematical Formulation

Some approaches are used to facilitate the solution of governing equations. One of them is the Boussinesq approach. In this approach, all other fluid transport properties are considered constant, except for the change in density. The equations written according to this approach are given below.

In steady state conditions, for three-dimensional laminar incompressible flow, continuity, momentum and energy equations in Cartesian coordinates can be written as follows.

Continuity equation;

$$\frac{\partial u}{\partial x} + \frac{\partial v}{\partial y} + \frac{\partial w}{\partial z} = 0 \quad (1)$$

x-momentum equation;

$$u \frac{\partial u}{\partial x} + v \frac{\partial u}{\partial y} + w \frac{\partial u}{\partial z} = -\frac{1}{\rho} \frac{\partial p}{\partial x} + \nu \left(\frac{\partial^2 u}{\partial x^2} + \frac{\partial^2 u}{\partial y^2} + \frac{\partial^2 u}{\partial z^2} \right) \quad (2)$$

y-momentum equation;

$$u \frac{\partial v}{\partial x} + v \frac{\partial v}{\partial y} + w \frac{\partial v}{\partial z} = -\frac{1}{\rho} \frac{\partial p}{\partial y} + \nu \left(\frac{\partial^2 v}{\partial x^2} + \frac{\partial^2 v}{\partial y^2} + \frac{\partial^2 v}{\partial z^2} \right) + \beta g(T - T_0) \quad (3)$$

z-momentum equation;

$$u \frac{\partial w}{\partial x} + v \frac{\partial w}{\partial y} + w \frac{\partial w}{\partial z} = -\frac{1}{\rho} \frac{\partial p}{\partial z} + \nu \left(\frac{\partial^2 w}{\partial x^2} + \frac{\partial^2 w}{\partial y^2} + \frac{\partial^2 w}{\partial z^2} \right) \quad (4)$$

In these equations, p represents pressure, ν kinematic viscosity and ρ density.

Energy equation;

$$u \frac{\partial T}{\partial x} + v \frac{\partial T}{\partial y} + w \frac{\partial T}{\partial z} = \alpha \left(\frac{\partial^2 T}{\partial x^2} + \frac{\partial^2 T}{\partial y^2} + \frac{\partial^2 T}{\partial z^2} \right) \quad (5)$$

Here; $\alpha = k/\rho c_p$ is the thermal diffusion coefficient and viscous dissipation is neglected. Transport properties of the fluid have been accepted as constant. These assumptions necessarily bring some errors. However, the fact that the temperature changes are not excessive prevents these errors to be large.

The expression $\beta g(T - T_0)$ in the equation (3) above is defined as the term related to the buoyancy force,

and indicates the acceleration of the fluid due to natural convection. T_0 indicates the inlet temperature

3.1. Boundary conditions

Inlet boundary conditions;

$$u_{z=0} = 0, v_{z=0} = 0, w_{z=0} = w_0, T_{z=0} = T_0, p_{z=0} = p_0 \quad (6)$$

Outlet boundary conditions;

Assuming that the length of the channel is long enough, it can be written that the changes of the dependent variables in the direction of the channel axis at the output are zero.

$$\left. \frac{\partial T}{\partial z} \right|_{z=L} = 0, \quad \left. \frac{\partial u}{\partial z} \right|_{z=L} = 0, \quad \left. \frac{\partial v}{\partial z} \right|_{z=L} = 0, \quad \left. \frac{\partial w}{\partial z} \right|_{z=L} = 0 \quad (7)$$

Symmetry plane;

$$u_{x=0} = 0, \quad \left. \frac{\partial v}{\partial x} \right|_{x=0} = 0, \quad \left. \frac{\partial w}{\partial x} \right|_{x=0} = 0, \quad \left. \frac{\partial T}{\partial x} \right|_{x=0} = 0 \quad (8)$$

Side wall;

$$\left. \frac{\partial T}{\partial x} \right|_{x=W/2} = 0 \text{ (adiabatic)} \quad (9)$$

Assuming that there is no slippage on the upper, lower and side walls, conditions on these surfaces are written as given below;

$$u_{y=0} = 0, u_{y=H} = 0, u_{x=W/2} = 0 \quad (10)$$

$$v_{y=0} = 0, v_{y=H} = 0, v_{x=W/2} = 0 \quad (11)$$

$$w_{y=0} = 0, w_{y=H} = 0, w_{x=W/2} = 0 \quad (12)$$

Channel top surface;

$$-k \left. \frac{\partial T}{\partial y} \right|_{y=H} = \begin{cases} 0 & \text{adiabatic (for unheated surfaces)} \\ q_{conv}^* & \text{constant heat flux (for heated surfaces)} \end{cases} \quad (13)$$

Channel bottom surface;

$$-k \frac{\partial T}{\partial y} \Big|_{y=0} = \begin{cases} 0 & \text{adiabatic (for unheated surfaces)} \\ \dot{q}_{conv}'' & \text{constant heat flux (for heated surfaces)} \end{cases} \quad (14)$$

The non-dimensional numbers resulting from the above formulations are defined as
Hydraulic diameter;

$$Dh = \frac{4A}{P} \quad (15)$$

A: Channel cross-area (m²)

P: Channel perimeter (m)

Reynolds number;

$$Re = \frac{w_0 Dh}{\nu} \quad (16)$$

w₀: inlet velocity (m/s)

Grashof number;

$$Gr = \frac{g\beta(T_s - T_b)D_h^3}{\nu^2} \quad (17)$$

Modified Grashof number;

$$Gr^* = \frac{g\beta\dot{q}_{conv}''D_h^4}{k\nu^2} \quad (18)$$

g: Gravitational acceleration (m s⁻²)

β: Thermal expansion coefficient (K⁻¹)

q''_{conv}: Average convection heat flux (W/m²)

ν: Kinematic viscosity (m² s⁻¹)

Nusselt number can be calculated as shown below;

$$Nu_{D_h, upper j} = \frac{\dot{Q}_{conv, upper j} D_h}{A_{h, upper j} (\bar{T}_{s, upper j} - T_{bj}) k} \quad (19)$$

Nu: Nusselt number

Q̇_{conv}: Convection heat transfer (W)

D_h: Hydraulic diameter (m)

A_h: Surface area (m²)

T_s: Surface temperature (°C)

T_b: Local bulk temperature (°C)

k: Thermal conductivity of air (W/m K)

In a study conducted with the CFD method, the most important criterion is that the results are in agreement with an experimental study. In Figure 2, the results obtained from the experimental setup for mixed convection heat transfer from discrete heat sources placed in a three-dimensional rectangular channel were compared with the present numerical results, and the results were seen to be in agreement.

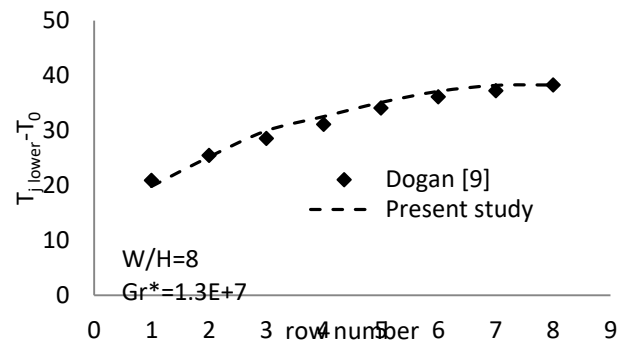


Figure 2. Comparison of numerical and experimental results for the lower heater temperatures for W/H = 8, Re = 971 and Gr* = 1.3x10⁷.

In Figure 3 (a) and (b), the change of Nusselt number according to the Grashof number is given for the value of W/H = 8 and Reynolds number 971 for upper and lower heaters, respectively.

As can be seen from the Figure 3 (a), the row averaged Nusselt number increased with the increase of Grashof number. In the inlet section of the channel the Nusselt number distributions show forced convection thermal entry region properties. The region where the buoyancy induced flow becomes dominant is described as the mixed convection region. For each Grashof number, Nusselt number decreases in the first four rows, and from the 5th row onwards, the Nusselt number increases along the channel, with the effect of the secondary flow. At the lower Grashof number of 5.8x10⁶ the secondary flow effects decreases, and the variation of the Nusselt number is more close to that for forced convection flow. When Nusselt number distributions in the upper part of the heaters are examined (Figure 3 (b)), forced convection behavior manifests itself, and there is a slight fluctuation in the last three rows. This is due to the fact that the fluid moving upward from the bottom affects the upper heaters.

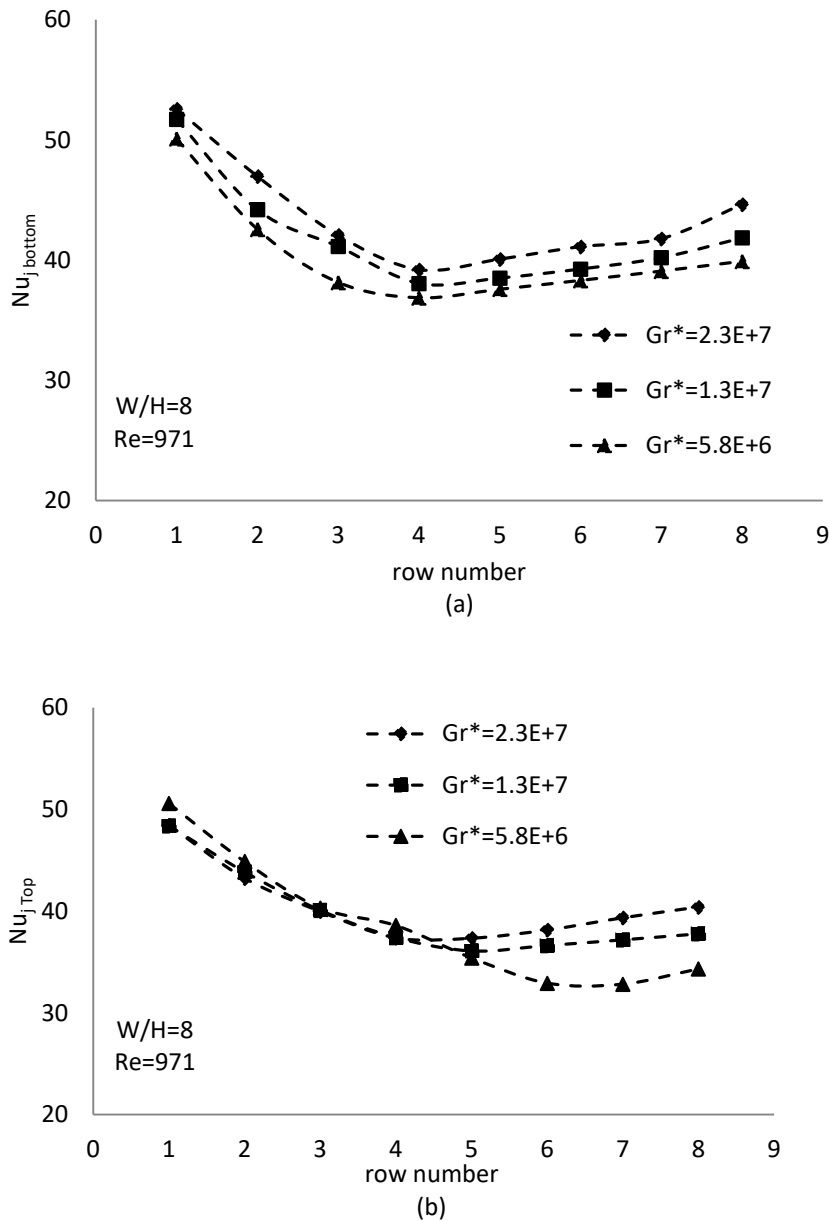


Figure 3. Nusselt number distributions for various modified Grashof numbers

Figure 4 (a) and (b) shows row averaged Nusselt number distributions for both upper and lower heaters for

different Reynolds numbers. As can be seen in Figure 4 (a), for all Reynolds numbers, the row averaged Nusselt numbers take a maximum value at the first rows, and from the 5th row, the buoyancy driven secondary flow has positive effects on the heat transfer, and as a result, Nusselt number increases. At 971, which is the maximum value of the Reynolds number, there is a decrease in the Nusselt number from the first row, but from the 5th row there is not much change on the Nusselt number along the channel. The higher the Reynolds number

the smaller are the fluctuations in the Nusselt number. Therefore, it can be said that the forced convection effects of Reynolds number at the maximum value of 971 are higher. Looking at the distribution of the Nusselt numbers in the upper part of the channel in Figure 4 (b), it can be said that the forced convection effects dominate under all Reynolds numbers. For minimum Reynolds number ($Re=150$), it was observed that there was not much change in the Nusselt numbers along the channel.

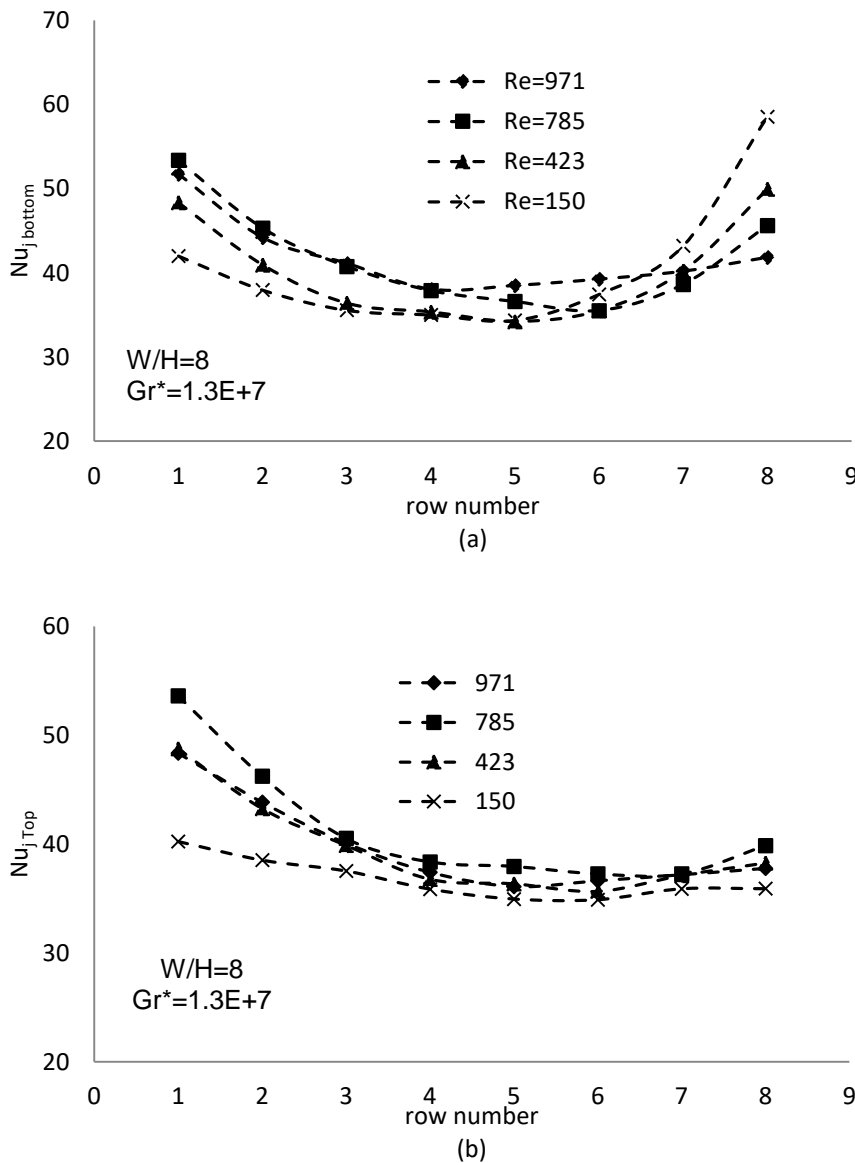
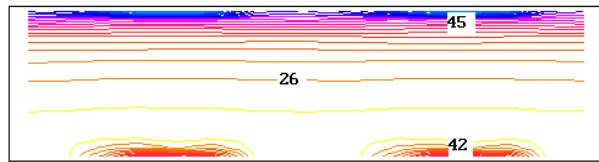


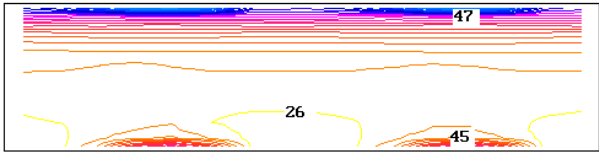
Figure 4. Nusselt number distributions for various Reynolds numbers

In Figure 5, temperature contour graphics are given for $W/H=8$ and $Gr=1.3 \times 10^7$. As can be seen in the figure, the upper heaters temperatures increase along the channel, but are higher than that of the lower heaters temperatures. When looking at the temperature contours, it is seen that the air rises and reaches maximum values at the upper part of the channel. It is seen that the fluid temperature is low in the middle part, since the middle part of the channel is under the influence of the main flow stream. The fluid temperature also increases along the channel depending on the surface temperatures.

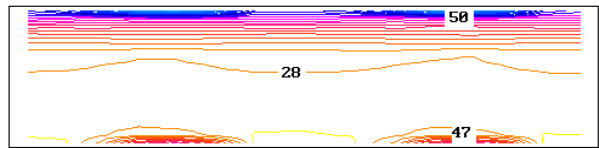
When looking at the vector velocity distributions in Figure 6, the vortex cycle is not very evident during the first heaters. It is observed that the velocity profiles did not deteriorate too much during the first heater and their vorticity was almost absent. It seems that instability begins at the second row and the flow is now completely disrupted throughout the channel. It was observed that the velocity profiles in the upper part did not change much. The local velocities are very small at the top of the channel at low speeds, causing the heaters to overheat.



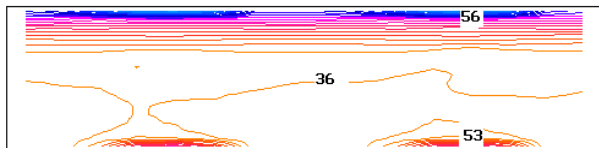
1st row



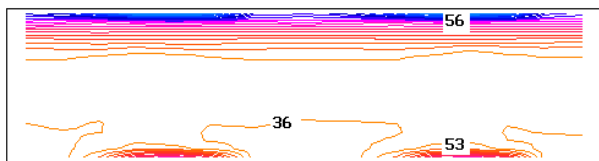
2nd row



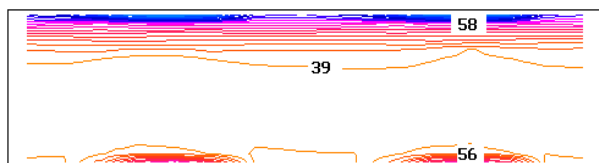
3rd row



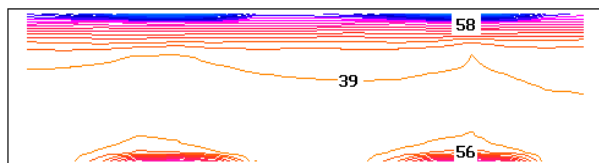
4th row



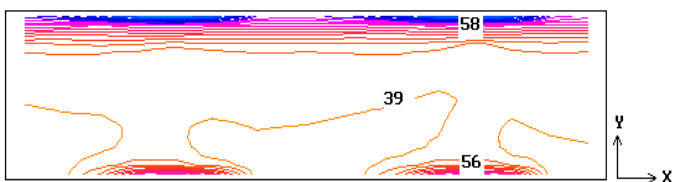
5th row



6th row

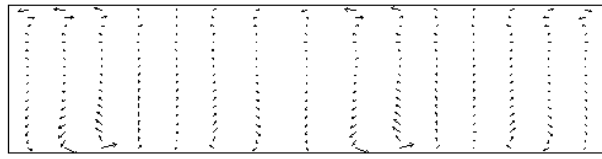


7th row

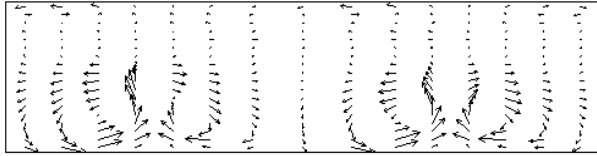


8th row

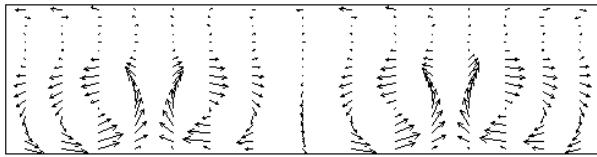
Figure 5. Temperature contour plots in the x-y plane for $Re_{Dh}=1459$, $W/H=8$, $Gr_{Dh}^*=1.3 \times 10^7$



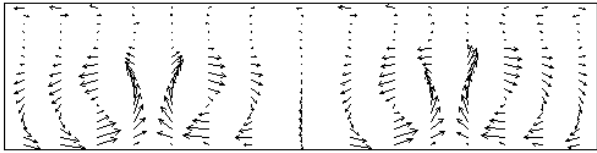
1st row



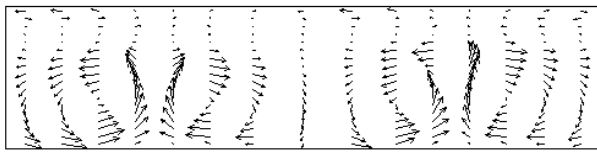
2nd row



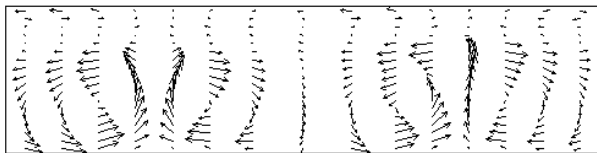
3rd row



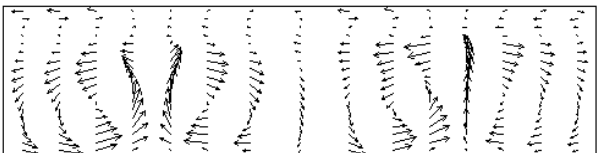
4th row



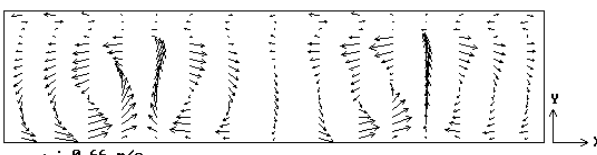
5th row



6th row



7th row



8th row

Figure 6. Vector velocity profiles in the x-y plane for $Re_{Dh}=1459$, $W/H=8$, $Gr_{Dh}^*=1.3 \times 10^7$

4. Conclusions

In this study, heat transfer under laminar mixed convection conditions in a horizontal channel with rectangular cross-section, discrete heaters with uniform heat flux on the upper and lower surfaces, was investigated numerically. For the heaters located in the lower part, the flow from the first row of the heaters has shown forced convection behavior, and an increase in the Nusselt numbers has been observed due to the effect of the secondary flow effective towards the middle rows (5, 6, 7, 8). For higher Grashof numbers, the buoyancy driven secondary flow was more effective. For higher Reynolds numbers, the Nusselt number has taken the maximum value, and forced convection effects have become more prominent. At the lower value of the Reynolds number, the difference between the Nusselt numbers for each row has decreased, and the secondary flow effect has become more dominant. The upper heaters, on the other hand, are mostly under the influence of the main stream, the forced convection feature outweighs and the Nusselt number is constantly decreasing throughout the number of rows. Only a slight increase was observed in the last row ($j = 8$). The reason for this increase is that the flow that moves upward from the bottom causes an intense air movement towards the heaters at the outlet. This situation caused an increase in the Nusselt number. For higher Grashof and lower Reynolds numbers, the elements at the upper channel were seen to be much warmer. This is undesirable. Especially in the design of electronic systems, placing the elements that emit low heat on the upper part is an important issue in terms of system security and efficiency.

References

- [1] Kennedy K. J., Zebib A., Combined free and forced convection between horizontal parallel planes: some case studies, *Int. J. Heat Mass Transfer.*, 26 (1983) 471–474.
- [2] Incropera F. P., Kerby J. S., Moffatt D. F., Ramadhyani S., Convection heat transfer from discrete heat sources in a rectangular channel. *Int. J. Heat Mass Transfer.*, 29 (1986) 1051–1058.
- [3] Choi C. Y., Ortega A., Mixed convection in an inclined channel with a discrete heat source, *Int. J. Heat Mass Transfer.*, 36 (1993) 3119–3134.
- [4] Mahaney H. V., Ramadhyani S., Incropera F. P., Numerical simulation of three-dimensional mixed convection heat transfer from an array of discrete heat sources in a horizontal rectangular duct., *Numer. Heat Transfer.*, 16 (1989) 267–286.
- [5] Dogan A., Sivrioglu M., Baskaya S., Experimental investigation of mixed convection heat transfer in a rectangular channel with discrete heat sources at the top and at the bottom, *Int. Commun. Heat Mass Transfer.*, 32 (2005) 1244–1252.
- [6] Özsunar A., Başkaya Ş., Sivrioglu M., Numerical analysis of Grashof number, Reynolds number inclination effects on mixed convection heat transfer in rectangular channels, *Int. J. of Comm. Heat Mass Transfer.*, 28 (2001) 985-994.
- [7] Amirouche Y., Bessaïh R., Numerical simulation of laminar mixed convection air-cooling from an array of heated electronic components mounted in a vertical channel, *International Renewable Energy Congress November 5-7, – Sousse, Tunisia.*, (2010) 268-275,
- [8] El Alami M., Najam M., Semma E., Oubarra A., Penot F., Electronic components cooling by natural convection in horizontal channel with slots, *Energy Conversion and Management.*, 46 (2005) 2762–2772.
- [9] Doğan A., Oney B., Experimental investigation of convection heat transfer from aluminum foam heat sinks, *Journal of the Faculty of Engineering and Architecture of Gazi University*, 29 (2014) 71-78.
- [10] Doğan A., Özbalcı O., Experimental Investigation of Free Convection from Foam Heat Sinks in an Inclined Rectangular Channel, *Cumhuriyet Sci. J.*, 39 (2018) 756-765.
- [11] Dogan A., Investigation of mixed convection heat transfer from a rectangular cross-section channel with discrete heat sources at the top and at the bottom, Ph.D. Thesis, Gazi University, Ankara, Turkey, (2003).
- [12] Rosten H., Spalding D. B., *The PHOENICS Beginners Guide*, London: CHAM I. Ltd, 1987.
- [13] Spalding D.B., *The PHOENICS Encyclopedia*, London: CHAM Ltd, 1994.